AGU PUBLICATIONS

JGR

Journal of Geophysical Research: Space Physics

RESEARCH ARTICLE
10.1002/2015JA021011

Key Points:
- Common periodicities are found in high-latitude pulsations and temperature
- The temperature variations are more evident during the dark polar winter
- The temperature is correlated with Pc5 and Pc1-2 power with a delay of few days

Correspondence to:
P. Francia,
patrizia.francia@aquila.infn.it

Citation:
Francia, P., M. Regi, and M. De Lauretis (2015), Signatures of the ULF geomagnetic activity in the surface air temperature in Antarctica, *J. Geophys. Res. Space Physics*, *120*, doi:10.1002/2015JA021011.

Received 14 JAN 2015
Accepted 21 FEB 2015
Accepted article online 24 FEB 2015

Signatures of the ULF geomagnetic activity in the surface air temperature in Antarctica

Patrizia Francia[1], Mauro Regi[1], and Marcello De Lauretis[1]

[1]Department of Physical and Chemical Sciences, University of L'Aquila, L'Aquila, Italy

Abstract The variations of the Pc5 and Pc1-2 ULF power and surface air temperature measured at Terra Nova Bay in Antarctica have been analyzed during the late declining phase of solar cycle 23 (2007–2008), in comparison with the simultaneous variations of the solar wind speed. The analysis focused on time scales of several days, which characterize the evolution of the solar wind stream structure. The temperature variations appear clearly during the local winters, while they are strongly reduced in the sunlit summers. During the local winters, the Pc5 and Pc1-2 power and the temperature variations are significantly correlated, with the temperature delayed by a few days with respect to the ULF power. A time-frequency analysis revealed common signals in the temperature and ULF power at periodicities related to the Sun's rotation period (~27, 13.5, and 9 days), which, in the same time intervals, characterize the solar wind speed and geomagnetic activity.

1. Introduction

The Sun affects the near-Earth space in a complex way, not only through solar radiation but also because of the solar wind (SW). In terms of energy, the SW energy input is extremely low, about a million times less than the solar radiative input [*Dudok de Wit and Watermann*, 2010]; however, due to its significant variations (by tens or hundred times during perturbed periods), it can play an important role in controlling the Earth's atmosphere. As a matter of fact, the SW variability, which reflects the variability of the solar atmosphere, manifests itself by different geoeffective structures through the solar cycle. Toward the minimum phase, high-speed SW streams originating from stable coronal holes interact periodically with the Earth's magnetosphere, producing recurrent geomagnetic activity [*Richardson et al.*, 2000]. The primary SW parameter that drives geomagnetic activity is the southward component B_z of the embedded interplanetary magnetic field (IMF), which may be observed in the interaction region between slow and fast wind, at the leading edge of the high-speed streams, and in the sheath regions ahead of the interplanetary coronal mass ejections and/or in the associated magnetic cloud; high values of the SW speed and density are also important in this context [*Pulkkinen et al.*, 2007, and references therein].

Geomagnetic activity has a significant influence on the Earth's upper and middle atmosphere, particularly at high latitudes, where energetic electrons from the radiation belts precipitate along the local geomagnetic field lines and changes of the polar cap electric potential difference occur.

The energetic particle precipitation can produce odd nitrogen (NO_x) which, during the polar winter, can live long enough to be transported into the stratosphere where it chemically perturbs the ozone distribution, altering the radiative balance in that region of the atmosphere; this eventually leads to detectable changes in surface air temperatures through dynamical coupling, with the whole process occurring on time scales of several weeks [*Rozanov et al.*, 2005; *Lu et al.*, 2008; *Seppala et al.*, 2009, 2013; *Baumgaertner et al.*, 2011].

In addition, the energetic particle precipitation can modify the electrical conductivity of the lower stratosphere, altering the current which flows from the ionosphere through the troposphere to the ground in the global electric circuit [*Tinsley and Zhou*, 2006; *Tinsley et al.*, 2007]. The current density J_z can also be modulated by an electric potential difference, determined by the VB_y component of the interplanetary electric field $V \times B$ (where V is the SW radial speed and B is the IMF), superimposed in the polar region to the uniform global potential [*Tinsley et al.*, 2007; *Burns et al.*, 2008].

In a pioneering work, *Markson* [1981] argued that an electrical mechanism in the lower stratosphere (such as the changes in the ionization and/or electric field induced by SW perturbations) could influence cloud physical processes through the release of latent heat, thus affecting atmospheric dynamics. This approach does not require energy transfer through the upper atmosphere and is characterized by a rapid response ($<$1 day).

More recent studies have shown that the current density changes could lead to variations in the cloud cover and lifetime, causing changes in the atmospheric radiative balance and dynamics [*Tinsley et al.*, 2007].

Using winter data from Vostok (at the altitude h~3.5 km on the Antarctic ice plateau), *Troshichev et al.* [2004] observed a warming (cooling) at ground level and a cooling (warming) at high altitudes ($h > 10$ km) in correspondence to a southward (northward) IMF rotation, with the effect reaching the maximum within 1 day and dampening equally quickly, while the temperature in the 4–8 km layer was practically invariant; they explained the results in terms of the formation of a cloud layer in the upper troposphere for $B_z < 0$, i.e., during geomagnetic perturbed conditions, which will efficiently back scatter the radiation going from the ice sheet so that the atmosphere would be hot below the cloud layer and would be cool above the layer. Moreover, *Troshichev et al.* [2008] found that in correspondence to a southward IMF rotation, there is an almost simultaneous increase of the cloud cover, followed by an increase of temperature at ground with a lag of 1–2 days.

Intense geomagnetic activity is characterized by the occurrence of ultralow frequency (ULF; ~1 mHz–10 Hz) fluctuations of the geomagnetic field lines, observed both in the magnetosphere and on the ground (see *Menk* [2011] for a review). In particular, lower-frequency waves (Pc5 pulsations, ~1–7 mHz) are energized by the SW through several mechanisms, ranging from wave generation by Kelvin-Helmholtz instability at the SW-magnetosphere boundary to direct penetration into the magnetosphere of waves contained in the interaction regions at the leading edges of the SW high-speed streams [*Regi et al.*, 2015]. In recent years, Pc5 waves have received considerable attention regarding their role in accelerating to relativistic energy magnetospheric electrons, particularly in the outer radiation belt [*Baker et al.*, 1998; *Rostoker et al.*, 1998; *Mathie and Mann*, 2000; *Mann et al.*, 2004]. *Rostoker et al.* [1998] observed, throughout a 90 day interval, that increases in energetic electron fluxes at geosynchronous orbit are always preceded by increases in the Pc5 wave activity at high latitude by 1–2 days. *Mathie and Mann* [2000] showed that significant geosynchronous electron flux enhancements appeared in response to extended intervals of enhanced Pc5 wave power at auroral stations, associated with high-speed SW streams. The highest correlation between SW speed, Pc5 wave power, and MeV electron flux was found in the declining phase of the solar cycle [*Mann et al.*, 2004]. The acceleration process is believed to involve resonant interaction of the Pc5 electric and magnetic field oscillations with the electron drift motion outside geosynchronous orbit, leading to radial inward transport [*Elkington*, 2006; *Hudson et al.*, 2008].

In the meanwhile, *Rodger et al.* [2008] showed that the precipitation of 1 MeV electrons into the atmosphere at L = ~4–5 was detected simultaneously with electromagnetic ion cyclotron (EMIC) wave activity observed by ground-based magnetometers. EMIC waves occur in the ULF higher-frequency range (Pc1-2 pulsations, 0.1–5 Hz) and are generated near the magnetic equator by unstable distributions of ring current ions during geomagnetic storms [*Menk*, 2011, and references therein]. Theoretical studies have demonstrated that such waves should be an effective mechanism for loss of >1 MeV electrons from the radiation belts through pitch angle scattering by gyroresonant interaction [*Engebretson et al.*, 2008, and references therein]; the results by *Rodger et al.* [2008] were consistent with precipitation occurring near the plasmapause, where EMIC waves may resonate with relativistic electrons.

In this study, we investigated the connection between geomagnetic disturbances and atmospheric effects during 2007–2008, at the last declining phase of the solar cycle 23, which was characterized by recurrent geomagnetic activity, associated with SW high-speed streams emanating from low-latitude coronal holes on the Sun [*Gibson et al.*, 2009]. We focused our attention on the possible relationship of the ULF geomagnetic activity with the surface air temperature measured at high latitude and investigated the occurrence of common periodicities in the SW speed, ULF geomagnetic power (in both the Pc5 and Pc1-2 frequency bands), and surface air temperature. We analyzed time scales from days up to few tens of days over which the SW stream structure is observed to evolve. The analysis shows a significant relationship between the ULF wave power and the surface air temperature and a close correspondence between their variations at the 27 day solar synodic rotation period and subharmonics.

2. Data Analysis

To study the geomagnetic activity variations, we used the power of ULF geomagnetic field fluctuations measured in Antarctica, at Mario Zucchelli base (Terra Nova Bay, 80°S) during 2007–2008. The instrumentation

consists of a low-power triaxial high-sensitivity search coil magnetometer recording at once the northward (*H*), eastward (*D*), and vertically downward (*Z*) components of the geomagnetic field variations. The power spectral density has been evaluated over 60 min intervals and then integrated in the range of ~1–7 mHz and ~100–500 mHz in order to obtain the total power in the Pc5 and Pc1-2 frequency bands, respectively. The ULF power typically undergoes strong, impulsive enhancements of several orders of magnitude, and then we use the logarithm of this quantity as a more suitable index for the ULF activity.

The surface air temperature measurements are carried out, at a sample interval of 1 h, at the automatic weather station Eneide, located at Terra Nova Bay, during the same years.

We also used 60 min averages of the SW speed from the OMNIWeb database (http://cdaweb.gsfc.nasa.gov/).

The basic data for our analysis are the daily averages of the SW speed, Pc5 and Pc1-2 power, and surface air temperature. The ULF power averages at Terra Nova Bay were computed excluding the hours close to the local magnetic noon (i.e., 18:00–22:00 UT, corresponding to 10:00–14:00 magnetic local time), when the station, which is at a latitude slightly higher than the auroral oval, approaches the cusp region, and measurements can be affected by the local ULF turbulence [*Engebretson et al.*, 1991; *Francia et al.*, 2009]. In addition, we preliminarily removed the mean value and the annual and semiannual modulations from both the temperature and ULF power averages.

We studied the time period evolution of the energy of common signals by applying the cross spectral analysis through the continuous wavelet transform [*Torrence and Compo*, 1998], more suitable than the traditional Fourier transform for analyzing nonstationary time series. We used the Morlet wavelet with nondimensional frequency equal to 6 so that the wavelet scale is almost equal to the Fourier period, and the time scale diagrams (scalograms) are almost identical to time period diagrams.

3. Experimental Results

The time series of the SW speed, the Pc5 power, the Pc1-2 power, and the surface air temperature during 2007–2008 are shown in Figure 1. Intense activity in the Pc5 and Pc1-2 bands is observed through the years, modulated by the SW stream occurrence. The surface air temperature is characterized by a reduced variability during the local summer (November–February), while during the winter months, its variations are remarkable and largely correspond to the variations of the ULF power and SW speed.

In order to quantitatively evaluate the relationship between the Pc5 and Pc1-2 power and the temperature, we performed a cross-correlation analysis of the mean-removed sequences, assuming the ULF power as input and the temperature as output, at different time lags (a negative/positive lag indicates that the input precedes/follows the output). Since the temperature fluctuations are strongly reduced during the local summer, we restricted our analysis to the local winter and equinoxes (April to September). The analysis was applied to 11 nonoverlapping time intervals, each one of 30 days. Then, we computed the average of the correlation coefficients obtained at each time lag. We evaluated the corresponding 90% confidence level through the Monte Carlo test by applying 10,000 times the same cross-correlation procedure to independent, red noise (modeled by a first order, autoregressive AR1 process) data series. The results shown in Figure 2 indicate that the temperature is significantly correlated (r~0.4) with the Pc1-2 power at a time lag of −1 day. Although lower, the correlation with the Pc5 power is also significant, reaching the maximum value when the temperature is delayed by 3 days with respect to the Pc5 power. From the Monte Carlo simulation, we also estimated P values of 0.0011 for the Pc1-2 power and 0.0354 for the Pc5 power at the time lags of the maximum correlation, indicating, respectively, strong and moderate evidence against the null hypothesis in favor of the relationship.

We found it interesting to estimate the amplitude of the temperature response to the variations of the Pc1-2 power. In Figure 3, we show the scatterplot of the temperature versus the Pc1-2 power as well as the comparison between the predicted values resulting from the best fit analysis and the experimental temperatures. The temperature data were shifted by the observed 1 day delay. Taking into account that the pulsation power follows a normal distribution, we excluded the data in the tails of the distribution (outside three standard deviations), thus improving the correlation (r ~ 0.5). Actually, we found that for most of the time, the temperature fluctuations estimated by the linear regression analysis correspond

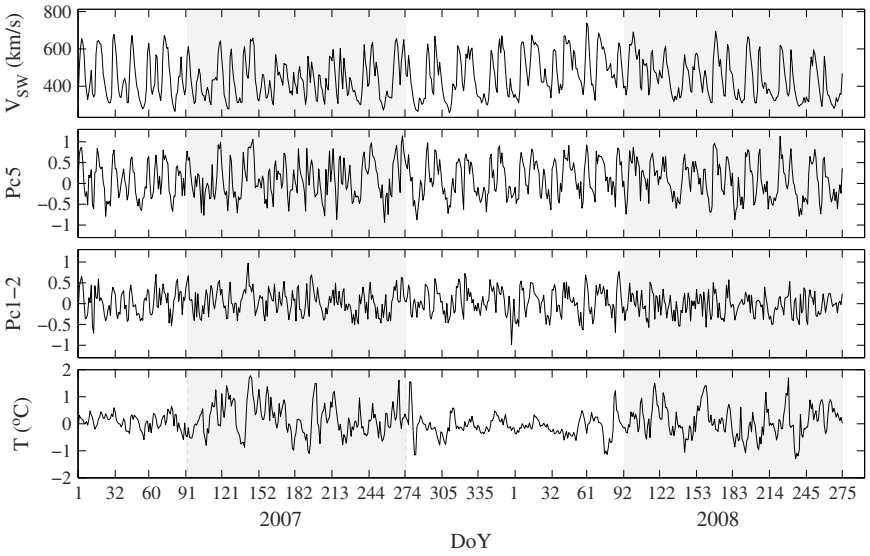

Figure 1. The daily averages of the SW speed, Pc5 power, Pc1-2 power, and surface air temperature at Terra Nova Bay during 2007–2008. The labels on the *x* axis indicate the first day of odd months, and the shaded areas mark the local winter months.

well to the experimental values although with a reduced amplitude, suggesting additional contributions to the temperature changes.

In order to study the degree of correspondence between pairs of parameters at different periodicities, we performed a cross wavelet spectral analysis [*Grinsted et al.*, 2004] which allows us to estimate the time period evolution of common features in the signals. In Figure 4, we show the amplitude of the cross spectra computed between the SW speed and the Pc5 and Pc1-2 power (top), the Pc5 power and the Pc1-2 power (middle), and finally the pulsation power and the temperature (bottom). The cross spectra involving the SW speed are roughly identical (they become different only after April 2008) and make clear the close correspondence of the SW speed signals at the periods of 27, 13.5, and 9 days (marked by dashed lines), corresponding to the solar rotation and its subharmonic periods, with those in the Pc5 and Pc1-2 power. This result confirms the well-established dependence of the ULF geomagnetic activity on the SW conditions. As a consequence, common features related to the SW speed are observed in the cross spectrum between the Pc5 power and the Pc1-2 power. As pointed out by several studies [*Lei et al.*, 2008b; *Tulasi Ram et al.*, 2010], the 27 day and subharmonic variations may be related to the longitudinal distribution of the coronal holes, from which the SW streams emanate, with one, two, or three equally spaced, long-lived holes producing the 27, 13.5, and 9 day periodicities in the SW speed. Finally, the cross spectra between the Pc5 and Pc1-2 power and the temperature appear similar, being characterized by amplitude enhancements at the same periodicities and during the same time intervals (except during the last months of 2008); the most interesting result is that such enhancements, emerging at the 27, 13.5, and 9 day periodicities, correspond quite well with most of those observed in the cross spectra between the SW speed and the Pc5 and Pc1-2 power, although with lower values.

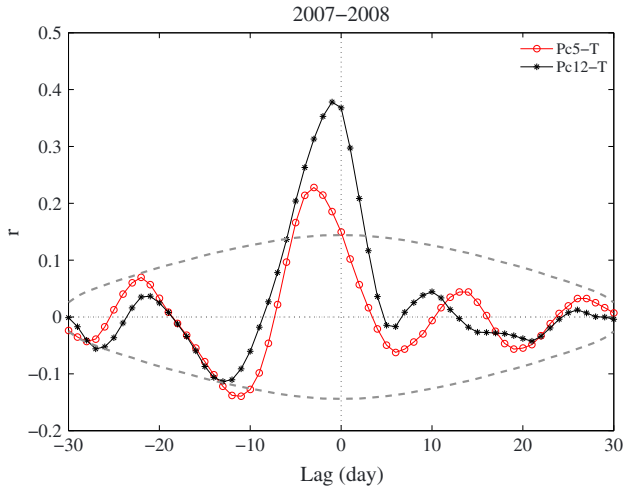

Figure 2. The cross correlation between the Pc5 and the Pc1-2 power and the temperature at different time lags. The dashed grey lines represent the 90% confidence level.

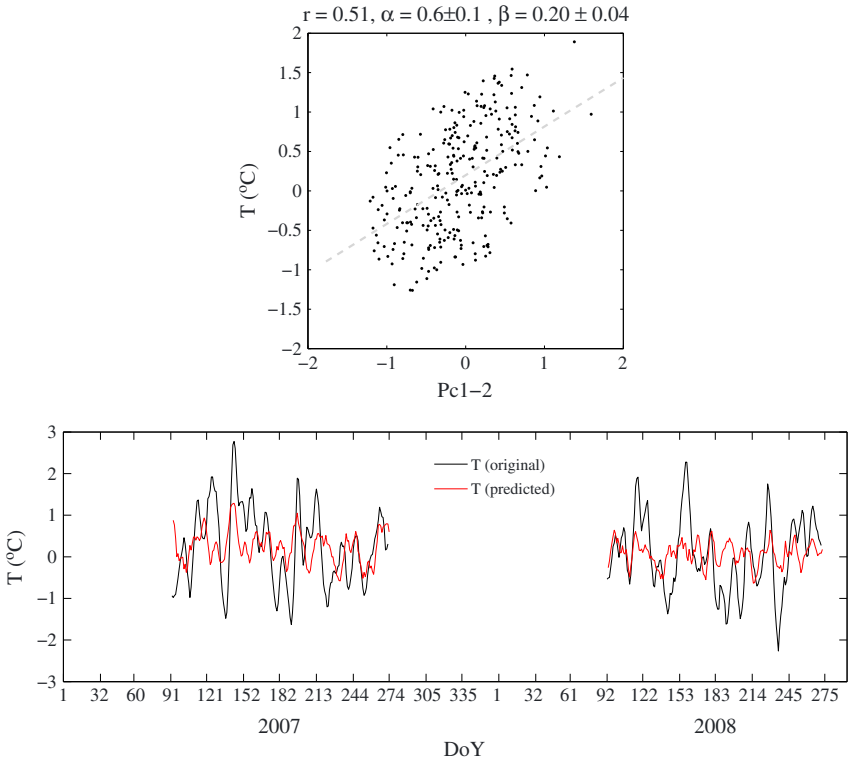

Figure 3. (top) The dependence of the temperature (1 day delayed) on the Pc1-2 power. The dashed line represents the linear regression. (bottom) The comparison between the original, experimental values of the temperature (black line) and the predicted ones (red line).

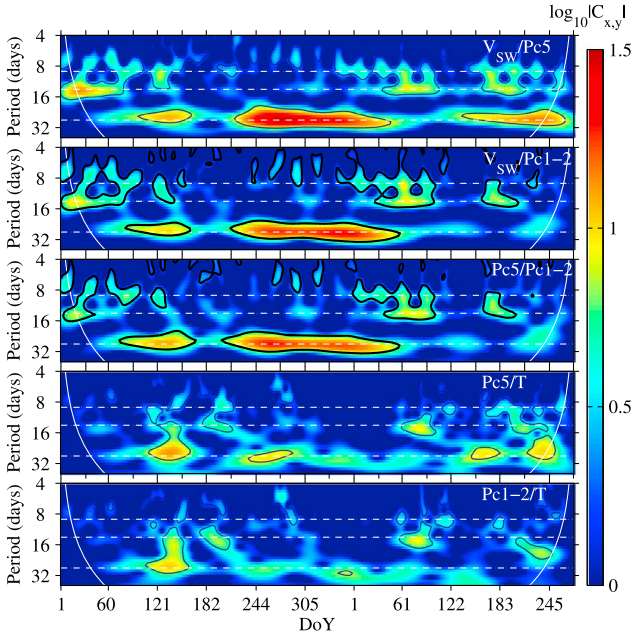

Figure 4. The cross spectra (top) between the SW speed and the Pc5 and Pc1-2 power, (middle) between the Pc5 power and Pc1-2 power, and (bottom) between the Pc5 and Pc1-2 power and the surface air temperature. The black contours encircle significant energy above the 90% confidence level.

We made a more accurate investigation of the time period relationship between the Pc5 (Pc1-2) power and the temperature performing the wavelet coherence analysis [*Grinsted et al.*, 2004]; it represents a normalized measure which can reveal features even though the common power is low. In Figure 5, we show the coherence and phase for the pairs Pc5 power-temperature (top) and Pc1-2-temperature (bottom). We can see that the coherence reaches values above the significance level at approximately the same times and periodicities characterized by high values of the cross spectra, and in addition, it reveals features that are not evident in the cross spectra, mostly at periodicities smaller than 9 days. If we focus our attention on the significant regions, the phase angle appears fairly constant and generally with a nonzero, negative value, indicating that the temperature fluctuations follow the ULF

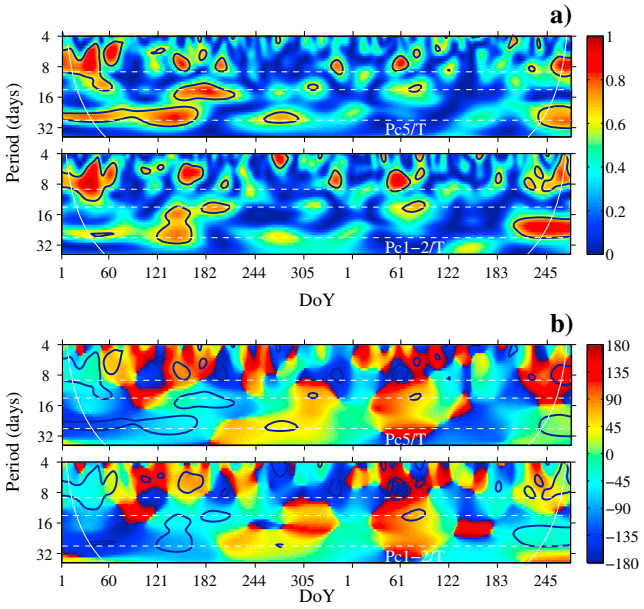

Figure 5. (a) Squared wavelet coherence (top) between the Pc5 power and the surface air temperature and (bottom) between the Pc1-2 power and the surface air temperature. (b) Phase difference (degrees) (top) between the Pc5 power and the surface air temperature and (bottom) between the Pc1-2 power and the surface air temperature. The black contours encircle values above the 90% confidence level.

power variations. It is worth to note that in some cases, the phase shows a positive, generally small, value, indicating a preceding temperature; this opposite behavior, consistent with the positive time lags observed for few cross-correlation values above the confidence level (Figure 2), probably reflects the variable contribution of the different inputs which affect the temperature.

4. Summary and Conclusions

In this study we investigated the possible relationship between the ULF geomagnetic activity and the surface air temperature measurements. For this scope, we analyzed the magnetic and temperature measurements at Terra Nova Bay, in Antarctica, during the years 2007–2008 characterized by recurrent high-speed SW streams [*Gibson et al.*, 2009].

Pc5 and Pc1-2 waves in the outer magnetosphere, where they are assumed, respectively, to accelerate electrons and to cause their precipitation, can propagate almost instantaneously to the ground at high latitudes [*Menk*, 2011]. Thus, the measurement of pulsations at Terra Nova Bay can be considered as a remote sensing of such magnetospheric waves; as matter of fact, in a recent analysis [*Regi et al.*, 2015], we found that enhancements of the Pc5 power at ground and geosynchronous orbit (GOES 12) occur almost simultaneously (within 3 h).

Interestingly, we obtained that restricting the analysis to the local winter when a strong variability is observed in the surface air temperature [see also *Yu et al.*, 2011], the time series of the pulsation power and temperature appear significantly correlated, with the temperature delayed by a few days. The correlation is higher with the Pc1-2 power than with the Pc5 power, as can be expected since, while the Pc5 pulsations have a role in the acceleration of the electrons, atmospheric changes are directly related to the energetic electron precipitation caused by the Pc1-2 pulsations.

The short delays by which the temperature follows the Pc5 and Pc1-2 power (3 days and 1 day, respectively) are comparable to those observed, respectively, between the Pc5 power increases and geosynchronous energetic electron flux enhancements [*Baker et al.*, 1998; *Rostoker et al.*, 1998; *Mathie and Mann*, 2000; *Mann et al.*, 2004] and between the Pc1-2 intensification and the precipitation of 1 MeV electrons into the atmosphere at $L = \sim 4–5$ [*Rodger et al.*, 2008]. They are also consistent with the results of the analyses conducted by *Troshichev et al.* [2004, 2008], who found an almost instantaneous (within 1–2 days) response of the ground temperature at Vostok to the IMF variations.

We observed a close correspondence between the temperature and ULF power at periodicities related to the Sun's synodic rotation period, i.e., at ~27, 13.5, 9, and 7 days, very similar to that observed between the pulsation power and the SW speed during the same time intervals. Further evidence of the connection between the two phenomena would be a phase-locked behavior; in our case, the phase difference is fairly constant at the observed periodicities and indicates that the temperature is generally delayed with respect to the ULF power (consistently with the correlation analysis); however, in some cases, it is found the opposite behavior, which suggests that additional processes might contribute to the temperature changes at the same periodicities (and thus, mainly of solar origin).

The same periodicities were reported by several authors [*Lei et al.*, 2008a; *Tayer et al.*, 2008; *Tulasi Ram et al.*, 2010] in the SW speed, in the coronal hole areas where the SW streams are rooted, in the geomagnetic activity index *Kp*, and in the thermosphere/ionosphere system during the declining phase of the solar cycle 23. Moreover, it is worth to note that *Yu et al.* [2011], using a 29 year reanalysis data set, revealed the existence of two major oscillations with periods of 26–30 days and 14 days in the surface air temperature in Antarctica during the local winter.

Evidence for atmospheric dynamical responses, through cloud physical processes, to current density changes in the global electric circuit has been clearly found, and SW related energetic electron precipitation and polar cap ionospheric convection potential changes have been observed as short-term inputs to such circuit [*Tinsley et al.*, 2007; *Burns et al.*, 2008]. The electron precipitation and the polar cap ionospheric potential changes are usually associated to perturbed geomagnetic conditions and, as previously discussed, to intense ULF activity.

Our results, i.e. the significant correlation between the high latitude ground temperature and the Pc5 and Pc1-2 power, particularly at the synodic periodicities, and the corresponding few day time delays, are consistent with the process of acceleration by Pc5 waves and precipitation by Pc1-2 waves of energetic electrons from the radiation belts and support the electrical mechanism as the possible coupling process between SW-driven geomagnetic perturbations and the low-atmosphere conditions.

Acknowledgments

This research activity was supported by the Italian PNRA (Programma Nazionale di Ricerche in Antartide). It was performed in relation with the European program COST ES1005. Measurements of the magnetic field fluctuations at Terra Nova Bay can be requested to Marcello De Lauretis at the following e-mail address: marcello.delauretis@aquila.infn.it. Temperature data were obtained from "Meteo-Climatological Observatory" of PNRA (www.climantartide.it). The authors acknowledge J.H. King and N. Papatashvilli at NASA and CDAWeb for the solar wind data.

Alan Rodger thanks Sabiuddin Mufti and another reviewer for their assistance in evaluating this paper.

References

Baker, D. N., T. I. Pulkkinen, K. X. Li, and S. G. Kanekal (1998), Coronal mass ejections, magnetic clouds, and relativistic magnetospheric electron events: ISTP, *J. Geophys. Res.*, *103*, 17,279–17,291, doi:10.1029/97JA03329.

Baumgaertner, A. J. G., A. Seppala, P. Jockel, and M. A. Clilverd (2011), Geomagnetic activity-related NO_x enhancements and polar surface air variability in a chemistry climate model: Modulation of the NAM index, *Atmos. Chem. Phys.*, *11*, 4521–4531.

Burns, G. B., B. A. Tinsley, W. J. R. French, O. A. Troshichev, and A. V. Frank-Kamenetsky (2008), Atmospheric circuit influences on ground-level pressure in the Antarctic and Arctic, *J. Geophys. Res.*, *113*, D15112, doi:10.1029/2007JD009618.

Dudok de Wit, T., and J. Watermann (2010), Solar forcing of the terrestrial atmosphere, *C. R. Geosci.*, *342*, 259–272.

Elkington, S. R. (2006), A review of ULF interactions with radiation belt electrons, in *Magnetospheric ULF Waves: Synthesis and New Directions*, *Geophys. Monogr.*, vol. 169, 177–193, AGU, Washington, D. C., doi:10.1029/169GM12.

Engebretson, M. J., L. J. Cahill Jr., R. L. Arnoldy, B. J. Anderson, T. J. Rosenberg, D. L. Carpenter, U. S. Inan, and R. H. Eather (1991), The role of the ionosphere in coupling upstream ULF wave power into the dayside magnetosphere, *J. Geophys. Res.*, *96*, 1527–1542, doi:10.1029/90JA01767.

Engebretson, M. J., et al. (2008), Pc1-2 waves and energetic particle precipitation during and after magnetic storms: Superposed epoch analysis and case studies, *J. Geophys. Res.*, *113*, A01211, doi:10.1029/2007JA012362.

Francia, P., M. De Lauretis, M. Vellante, U. Villante, and A. Piancatelli (2009), ULF geomagnetic pulsations at different latitudes in Antarctica, *Ann. Geophys.*, *27*, 3621–3629.

Gibson, S. E., J. U. Kozyra, G. de Toma, B. A. Emery, T. Onsager, and B. J. Thompson (2009), If the Sun is so quiet, why is the Earth ringing? A comparison of two solar minimum intervals, *J. Geophys. Res.*, *114*, A09105, doi:10.1029/2009JA014342.

Grinsted, A., J. C. Moore, and S. Jevrejeva (2004), Application of the cross wavelet transform and wavelet coherence to geophysical time series, *Nonlinear Processes Geophys.*, *11*, 561–566.

Hudson, M. K., B. Kress, H. Mueller, J. Zastrow, and J. Bernardblake (2008), Relationship of the Van Allen radiation belts to solar wind drivers, *J. Atmos. Sol. Terr. Phys.*, *70*, 708–729.

Lei, J., J. P. Thayer, J. M. Forbes, E. K. Sutton, R. S. Nerem, M. Temmer, and A. M. Veronig (2008a), Global thermospheric density variations caused by high-speed solar wind streams during the declining phase of solar cycle 23, *J. Geophys. Res.*, *113*, A11303, doi:10.1029/2008JA013433.

Lei, J., J. P. Thayer, J. M. Forbes, Q. Wu, C. She, W. Wan, and W. Wang (2008b), Ionosphere response to solar wind high-speed streams, *Geophys. Res. Lett.*, *35*, L19105, doi:10.1029/2008GL035208.

Lu, H., M. A. Clilverd, A. Seppala, and L. L. Hood (2008), Geomagnetic perturbations on stratospheric circulation in late winter and spring, *J. Geophys. Res.*, *113*, D16106, doi:10.1029/2007JD008915.

Mann, I. R., T. P. O'Brien, and D. K. Milling (2004), Correlations between ULF wave power, solar wind speed, and relativistic electron flux in the magnetosphere: Solar cycle dependence, *J. Atmos. Sol. Terr. Phys.*, *66*, 187, doi:10.1016/j.jastp.2003.10.002.

Markson, R. (1981), Modulation of the Earth's electric field by cosmic radiation, *Nature*, *291*, 304–308.

Mathie, R. A., and I. R. Mann (2000), A correlation between extended intervals of ULF wave power and storm-time geosyncronous relativistic electron flux enhancements, *Geophys. Res. Lett.*, *27*, 3261–3264, doi:10.1029/2000GL003822.

Menk, F. W. (2011), Magnetospheric ULF waves: A review, in *The Dynamic Magnetosphere, IAGA Spec. Sopron Book Ser.*, vol. 3, edited by W. Liu and M. Fujimoto, pp. 223–256, Springer, Berlin.

Pulkkinen, T. I., M. Palmroth, E. I. Tanskanen, N. Y. Ganushkina, M. A. Shukhtina, and N. P. Dmitrieva (2007), Solar wind-magnetosphere coupling: A review of recent results, *J. Atmos. Sol. Terr. Phys.*, *69*, 256–264, doi:10.1016/j.jastp.2006.05.029.

Regi, M., M. De Lauretis, and P. Francia (2015), Pc5 geomagnetic fluctuations in response to solar wind excitation and their relationship with relativistic electron fluxes in the outer radiation belt, *Earth Planets Space*, *67*, 9, doi:10.1186/s40623-015-0180-8.

Richardson, I. G., E. W. Cliver, and H. V. Cane (2000), Sources of geomagnetic activity over the solar cycle: Relative importance of coronal mass ejections, high-speed streams, and slow solar wind, *J. Geophys. Res.*, *105*, 18,203–18,213, doi:10.1029/1999JA000400.

Rodger, C. J., T. Raita, M. A. Clilverd, A. Seppala, S. Dietrich, N. R. Thomson, and T. Ulich (2008), Observations of relativistic electron precipitation from the radiation belts driven by EMIC waves, *Geophys. Res. Lett.*, *35*, L16106, doi:10.1029/2008GL034804.

Rostoker, G., S. Skone, and D. N. Baker (1998), On the origin of relativistic electrons in the magnetosphere associated with some geomagnetic storms, *Geophys. Res. Lett.*, *25*, 3701–3704, doi:10.1029/98GL02801.

Rozanov, E., L. Callis, M. Schlesinger, F. Yang, N. Andronova, and V. Zubov (2005), Atmospheric response to NO_y source due to energetic electron precipitation, *Geophys. Res. Lett.*, *32*, L14811, doi:10.1029/2005GL023041.

Seppala, A., C. E. Randall, M. A. Clilverd, E. Rozanov, and C. J. Rodger (2009), Geomagnetic activity and polar surface air temperature variability, *J. Geophys. Res.*, *114*, A10312, doi:10.1029/2008JA014029.

Seppala, A., H. Lu, M. A. Clilverd, and C. J. Rodger (2013), Geomagnetic activity signatures in wintertime stratosphere wind, temperature, and wave response, *J. Geophys. Res. Atmos.*, *118*, 2169–2183, doi:10.1002/jgrd.50236.

Tayer, J. P., J. Lei, J. M. Forbes, E. K. Sutton, and R. S. Nerem (2008), Thermospheric density oscillations due to periodic solar wind high-speed streams, *J. Geophys. Res.*, *113*, A06307, doi:10.1029/2008JA013190.

Tinsley, B. A., and L. Zhou (2006), Initial results of a global circuit model with stratospheric and tropospheric aerosols, *J. Geophys. Res.*, *111*, D16205, doi:10.1029/2005JD006988.

Tinsley, B. A., G. B. Burns, and L. Zhou (2007), The role of the global electric circuit in solar and internal forcing of clouds and climate, *Adv. Space Res.*, *40*, 1126–1139, doi:10.1016/j.asr.2007.01.071.

Torrence, C., and G. P. Compo (1998), A practical guide to wavelet analysis, *Bull. Am. Meteorol. Soc.*, *79*, 61–78.

Troshichev, O., L. V. Egorova, and V. Y. Vovk (2004), Influence of the solar wind variations on atmospheric parameters in the southern polar region, *Adv. Space Res.*, *34*, 1824–1829, doi:10.1016/j.asr.2003.06.034.

Troshichev, O., V. Vovk, and L. Egorova (2008), IMF-associated cloudiness above near-pole station Vostok: Impact on wind regime in winter Antarctica, *J. Atmos. Sol. Terr. Phys.*, *70*, 1289–1300, doi:10.1016/j.jastp.2008.04.003.

Tulasi Ram, S., C. H. Liu, and S.-. Y. Su (2010), Periodic solar wind forcing due to recurrent coronal holes during 1996–2009 and its impact on Earth's geomagnetic and ionospheric properties during the extreme solar minimum, *J. Geophys. Res.*, *115*, A12340, doi:10.1029/2010JA015800.

Yu, L., Z. Zhang, M. Zhou, S. Zhong, B. Sun, H. Hsu, Z. Gao, H. Wu, and J. Ban (2011), The intraseasonal variability of winter semester surface air temperature in Antarctica, *Polar Res.*, *30*, 6039, doi:10.3402/polar.v30i0.6039.